Modeling saturated and unsaturated ferroelectric hysteresis loops: An analytical approach

C. H. Tsang and C. K. Wong[a]
Department of Applied Physics, The Hong Kong Polytechnic University, Hong Kong, China

F. G. Shin
Department of Applied Physics, Materials Research Center and Center for Smart Materials,
The Hong Kong Polytechnic University, Hong Kong, China

In ferroelectric materials, hysteresis behavior is very difficult to model due to its nonlinear and history-dependent characteristics. Among approaches that are able to describe unsaturated loops, many of them are either very complicated (numerical procedures must be employed) or the resulting loops contain some undesirable or defective features. In this work, a simple hysteresis model based on a special construction of the Preisach function is proposed. Explicit expressions for the polarization-field (*P-E*) responses under increasing and decreasing applied fields have been derived. The saturated and unsaturated *P-E* loops can be conveniently calculated by piecing together such responses. The technique is widely applicable to the modeling of ferroelectric hysteresis behavior of ceramics and polymers. As examples we study the applied field dependence of dielectric permittivity of a ferroelectric film and the remanent polarization of ferroelectric composites after ac poling. We find that the model predictions agree well with the experimental results. © *2005 American Institute of Physics*. [DOI: 10.1063/1.2103417]

I. INTRODUCTION

Ferroelectrics are one of the most attractive materials due to their vast potential in different applications. In many applications, such as in precision machining, ferroelectric materials are required to operate under high electric fields. However, pronounced hysteresis behavior is evident in these conditions. In literature, there are many attempts of modeling ferroelectric hysteretic behavior under arbitrary fields, and often oversimplified empirical expressions are employed. Most approaches, despite their individual merits, are unable to satisfactorily and completely model hysteretic behavior in arbitrary applied fields. Miller *et al.* have proposed a useful differential hysteresis model which can simulate the polarization-field (*P-E*) response to deal with arbitrary applied field,[1] in which minor (unsaturated) loops are modeled by scaling the major (saturated) loop. However, the polarization is described by a differential equation without sufficient consideration of "history"-dependent effects so that unstable minor loops are produced.[2] On the other hand, the Preisach model,[3] well known in ferromagnetics, has been employed to study ferroelectrics,[4–6] and ferroelectric composites.[7] This model is based on the assumption that a ferroelectric consists of hysteretic units (hysterons) with a distribution of coercive fields described by a Preisach function. A shortcoming is the difficulty in obtaining explicit forms of the polarization (a double integral of the Preisach function) due to the complicated mathematical procedure.

Also, in characterizing the polarization behavior of a heterogeneous ferroelectric material, the gross polarization is mainly determined by the *P-E* response of the constituents,

their volume ratio, and the structure of interconnection for the different phases. The hysteresis of the constituents traces minor loops when the electric field acting on the constituents is not sufficiently large. Therefore, an explicit ferroelectric hysteresis model capable of simulating *P-E* relations in arbitrary fields is an essential tool to study the gross polarization response of a ferroelectric composite. On the other hand, studies of the applied field-dependent permittivity have attracted great research interest in the literature,[8–10] because ferroelectrics possessing high tunability of permittivity can be used in tunable device applications. In modeling such properties, one should note that the ferroelectric will also trace minor hysteresis loops under the small ac measuring field, which is superimposed on a dc electric field.

In this paper, we take the Preisach approach and introduce a superposition of Preisach functions. We have obtained explicit expressions of the polarization by choosing a special Preisach function for the Preisach integral which normally is very difficult to solve. This model is able to simulate polarization responses of many different combinations of applied fields. As examples, our hysteresis model is applied to study the electric-field dependence of permittivity in a ferroelectric film and the remanent polarization of ferroelectric 0-3 composites. Numerical simulation of the permittivity and the remanent polarization values is compared with the experimental data for a polyvinylidene fluoride (PVDF) polymer film,[11] and the triglycine sulfate/vinylidene fluoride-trifluoroethylene [TGS/P(VDF-TrFE)] 0-3 composites, respectively.[12] In general, the results agree well with the experiments. Discussion of our results with the predictions given by the model of Miller *et al.* will also be made. We
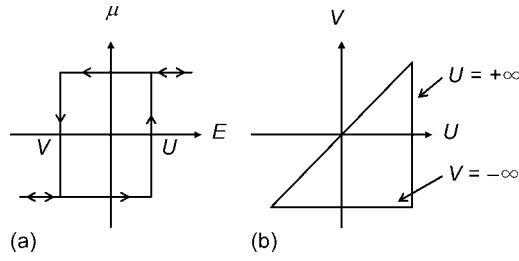
a)Electronic mail: wongck.ap@polyu.edu.hk

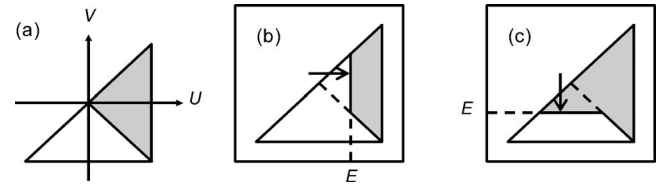FIG. 1. (a) A single Preisach hysteron, and (b) Preisach plane.

FIG. 2. (a) The status of the Preisach plane for a virgin material. The corresponding status of the Preisach plane for a virgin material after applying (b) an increasing field E and (c) a decreasing field E. The gray and white regions in the U-V plane denote regions in which $\mu=-1$ and $\mu=+1$, respectively.

will demonstrate that the presently proposed model is better suited for use to study the hysteresis behavior and dielectric tunability in ferroelectrics.

II. AN ANALYTICAL HYSTERESIS MODEL BASED ON THE PREISACH APPROACH

A. Classical Preisach model

The Preisach model was proposed in 1935. The model, transcribed for use in ferroelectrics, considers a material to be a collection of square-loop hysterons having two normalized spontaneous polarization states: $\mu=-1$ and $\mu=+1$, as shown in Fig. 1(a). Each hysteron is switched up if the external field E is increased to a value greater than the switch-up field U of the hysteron, and is switched down if the field is decreased to smaller than the switch-down field V of the hysteron.

An isolated hysteron has a well-defined coercive field, i.e., its P-E loop is symmetrically placed about $E=0$ (thus $U=-V$). Since hysterons would be subjected to interaction fields due to other hysterons inside the material, individual P-E hysteresis loops are shifted along the E axis. As a result, the magnitudes of the switching fields U and V may not be equal.

For an aggregation of hysterons, both U and V of individual hysterons may be distributed, the latter depend on their environment, leading to a distribution of U and V. This distribution represents therefore the distribution of hysterons, which characterizes a ferroelectric material, and is described by a Preisach function $\mathbf{P}(U,V)$. This function is defined over the Preisach plane, which is the U-V plane with $U \geqslant V$, as shown in Fig. 1(b). With this definition, all hysterons are switched up if a sufficiently large field E is applied to the material. Hence, the saturation polarization P_s equals the sum of the "switch-up" state of hysterons and is given by

$$P_s = \int\int_{U \geqslant V} \mathbf{P}(U,V)dUdV = \int_{-\infty}^{\infty}\int_{-\infty}^{U} \mathbf{P}(U,V)dVdU. \quad (1)$$

The polarization of a ferroelectric material generally is the sum of the integral of $\mathbf{P}(U,V)$ weighted by $\mu=+1$ and $\mu=-1$ depending on the field history. It follows that the Preisach plane is divided into two parts: S^+ where each hysteron has $\mu=+1$, and S^- where each hysteron has $\mu=-1$. Mathematically, the polarization is given by

$$P(E) = \int\int_{S^+} \mu(U,V)\mathbf{P}(U,V)dUdV$$
$$+ \int\int_{S^-} \mu(U,V)\mathbf{P}(U,V)dUdV$$
$$= \int\int_{S^+} \mathbf{P}(U,V)dUdV - \int\int_{S^-} \mathbf{P}(U,V)dUdV. \quad (2)$$

In this work, the normalized Preisach function $\wp(U,V;h,\nu)$ (i.e., $\mathbf{P}(U,V)/P_s$) is assumed to be a product of distributions of U and of V,

$$\wp(U,V;h,\nu) = \frac{1}{2\nu}\text{sech}\left(\frac{U-h}{\nu}\right)^2\left[1\right.$$
$$\left. - \tanh\left(\frac{U-h}{\nu}\right)\right]\frac{1}{2\nu}\text{sech}\left(\frac{V+h}{\nu}\right)^2$$
$$\times\left[1 - \tanh\left(\frac{V+h}{\nu}\right)\right], \quad (3)$$

where ν describes the dispersion of the distributions of U and of V. h is related to the maximum position of these distributions. Note that the expression for polarization depends on the history of the field applied onto the material. The advantage in choosing this function is that it can provide explicit forms for arbitrary polarization reversal curves, the virgin curve (from $P=0$), and major loop of a ferroelectric. According to Eq. (2), the polarization on the ascending major curve can be written as

$$P_{\text{sat}}^+(E;h,\nu) = -P_s + 2P_s\int_{-\infty}^{E}\int_{-\infty}^{U} \wp(U,V;h,\nu)dVdU, \quad (4)$$

and the polarization on the descending major curve as

$$P_{\text{sat}}^-(E;h,\nu) = P_s - 2P_s\int_{E}^{\infty}\int_{V}^{\infty} \wp(U,V;h,\nu)dUdV$$
$$= -P_{\text{sat}}^+(-E;h,\nu). \quad (5)$$

The closed form expression obtained by putting Eq. (3) into Eq. (4) is shown as Eq. (A1) in Appendix A. Now consider a virgin material on which a field E is applied. Since it starts from a state of zero polarization, we assume its initial state is well represented by the configuration shown in Fig. 2(a) on the Preisach plane, in which half of the hysterons are "up" and half are "down." Figures 2(b) and 2(c) show the corresponding status of the Preisach plane after applying E. If the
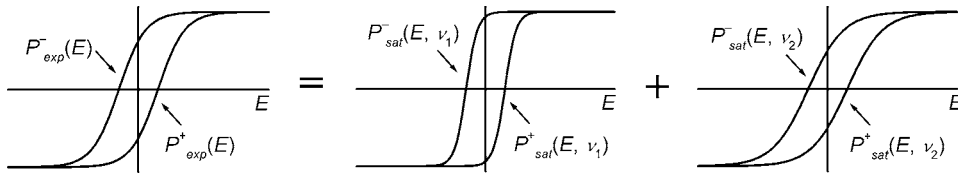
FIG. 3. An example of experimental hysteresis loop [i.e., $P_{exp}^{\pm}(E)$] is written as the sum of two Preisach-type hysteresis loops {i.e., $P_{sat}^{\pm}[E, h(\nu_i), \nu_i]$}.

applied field E is positive, then the polarization (on the virgin curve) is [see Fig. 2(b)]

$$P_0^+(E;h,\nu) = 2P_s \int_0^E \int_{-U}^U \wp(U,V;h,\nu) dV dU. \tag{6}$$

If the applied field E is negative, then the polarization (on the virgin curve) is [see Fig. 2(c)]

$$P_0^-(E;h,\nu) = 2P_s \int_0^E \int_V^{-V} \wp(U,V;h,\nu) dU dV$$

$$= -P_0^+(-E;h,\nu). \tag{7}$$

Assume that E_0 and E_1 are two successive extrema in the field history and $E_0 < E_1$. If now the applied field E increases from E_0 to E such that $E_0 \leq E < E_1$, then the change in the polarization is

$$\Delta P^+(E,E_0;h,\nu) = 2P_s \int_{E_0}^E \int_{E_0}^U \wp(U,V;h,\nu) dV dU. \tag{8}$$

The closed form expressions obtained by putting Eq. (3) into Eqs. (6) and (8) are shown as Eqs. (A3) and (A4) in Appendix A. Now assume that E_0 and E_1 are two successive extrema in the field history and $E_0 > E_1$. If the applied field E decreases from E_0 to E such that $E_0 \geq E > E_1$, then the change in the polarization is

$$\Delta P^-(E,E_0;h,\nu) = -2P_s \int_E^{E_0} \int_V^{E_0} \wp(U,V;h,\nu) dU dV$$

$$= -\Delta P^+(-E,-E_0;h,\nu). \tag{9}$$

Using Eqs. (4)–(9), the polarization of a ferroelectric for arbitrary field history can be calculated.

B. Superposition Preisach model

In the previous section, we see that an explicit form for the polarization of a ferroelectric under arbitrary field history can be obtained if the Preisach function of the material has the form of Eq. (3), which is a hyperbolic secant type (sech type) of distribution. It provides a convenient way to study the hysteretic behavior of the polarization of ferroelectrics. Experimental loops may also be modeled by other Preisach functions. For example, a Gaussian-Gaussian distribution has been employed to describe the hysteresis loops of TGS and P(VDF-TrFE) in a previous article.[7] The Preisach function of a lead zirconate titantate is described well by an exponential-exponential distribution.[13] Explicit expressions for the polarization are difficult to obtain for these distributions. Now to make use of Eq. (3) to describe a wider class of ferroelectrics, we propose to construct Preisach functions by summing a sequence of sech-type Preisach functions. Equivalently, a

polarization major loop is approximated by the sum of a sequence of polarization major loops with sech-type Preisach functions.

Consider the experimental ascending polarization major curve $P_{exp}^+(E)$ of a ferroelectric with spontaneous polarization P_s and coercive field E_c. Let $\wp_i(U,V;h,\nu_i)$ be a normalized sech-type Preisach function in the form of Eq. (3) with parameters h and ν_i, and $P_{sat}^+(E;h,\nu_i)$ be the ascending major curve calculated from Eq. (4). We assume that $P_{exp}^+(E)$ is approximated in the form of a sum of $P_{sat}^+(E;h,\nu_i)$ with weight factor k_i (see Fig. 3),

$$P_{exp}^+(E) = \sum_{i=1}^n k_i P_{sat}^+[E, h(\nu_i), \nu_i]. \tag{10}$$

$h(\nu) = \nu \ln \sqrt{1 - 2\cosh^2(-E_c/\nu) + 10\cosh(-E_c/\nu)\sqrt{\cosh^2(-E_c/\nu) - 1}}$ [which make the maximum of the derivative of $P_{sat}^+(E;h,\nu)$ occur at E_c]. n, k_i, and ν_i are chosen by fitting the experimental curve. Since the sech-type Preisach function [Eq. (3)] gives explicit expressions for arbitrary polarization reversal curves and the virgin curve, the simulated polarization curve under arbitrary field history and the simulated virgin curve for the ferroelectric can be expressed in analytical formulas. Moreover, this superposition method retains the properties of the classical Preisach model, e.g., the deletion property and congruency property.[14]

III. APPLICATIONS

A. Applied field dependence of dielectricity in PVDF

In this section, our model is applied to simulate the applied field dependence of dielectric permittivity in uniaxially drawn PVDF film measured by the methodology elaborated below. The dielectric constant of the film is also calculated by using an alternative definition of permittivity (i.e., the derivative of electric displacement with respect to the electric field) for comparison.

1. Methodology for measurement of dielectricity in PVDF

To investigate the linear dielectricity of ferroelectric polymers, Furukawa et al. proposed to use a double-frequency signal, in which a low field with high frequency was superimposed on a high field with low frequency, to measure the linear dielectric constant of ferroelectric polymer.[11] Mathematically, the applied field signal is

$$E = E_0 \cos \omega t + E_n \cos n\omega t, \tag{11}$$

where $\omega = 2\pi f$. Here the first term is the high field with low frequency, and the second term is the low field with high frequency. In the experiment of Furukawa et al.[11] they set $E_0 = 200$ V μm^{-1}, $f = 0.8$ Hz, $n = 128$, $E_n = E_0/10$, and N

TABLE I. The dielectric and ferroelectric properties, and the Preisach parameters k_i and ν_i of the PVDF sample used in Figs. 4 and 5.

ε_r	P_s (mC cm^{-2})	E_c (V μm^{-1})	k_1	ν_1 (V μm^{-1})	k_2	ν_2 (V μm^{-1})
9	80	75[a]	0.25	40	0.75	90

[a]Reference 11.

$=512$. N is the number of sampled data in the experiment for 1.25 s and m is defined as $N/n=4$. Then, averaging successive m data points in electric displacement D to get

$$D_0(J) = \sum_{K=1}^{m} D(mJ+K)/m, \quad J=1,\ldots,N/m, \quad (12)$$

which is the linear component of D. The $n\omega$ component (or nonlinear component) of D is obtained by using the Fourier technique. The corresponding Fourier coefficients are

$$D'_n = \frac{2}{m} \sum_{K=1}^{m} [D(mJ+K) - K\Delta D(J)]\cos(2\pi K/m), \quad (13)$$

and

$$D''_n = \frac{2}{m} \sum_{K=1}^{m} [D(mJ+K) - K\Delta D(J)]\sin(2\pi K/m), \quad (14)$$

where $\Delta D(J) = [D_0(J+1) - D_0(J-1)]/2m$. Thus, the $n\omega$ component is given by

$$D_n(J) = \sqrt{D'_n(J)^2 + D''_n(J)^2}. \quad (15)$$

$E_0(J)$ and $E_n(J)$ of $E(J)$ are obtained by using a similar procedure as for D. Then, the linear permittivity ε of the material is defined as

$$\varepsilon(J) = D_n(J)/E_n(J). \quad (16)$$

2. Comparison with the experimental dielectric permittivity of PVDF

We apply our model to investigate the dielectric permittivity measured under a bias field in uniaxially drawn PVDF film as commonly done in "dielectric tunability" studies. The applied electric field is traced by a schedule described by Eq. (11) and the electric displacement D of the sample is calculated by $\varepsilon_r\varepsilon_0 E + P$, where P is simulated by our superposition Preisach model. Then the D-E curve for each measurement in the experiment is Fourier analyzed (Sec. III A 1). The first-order in-phase components of the Fourier coefficients (i.e., linear permittivity) obtained are compared with the experimental data reported in Ref. 11. Table I shows all adopted values for the properties of the ferroelectric copolymer sample.[11] The Preisach parameters for the sample fitted from the steady-state major hysteresis loop are also shown in Table I. The D-E [here $D \equiv D_0(J)$ and $E \equiv E_0(J)$] for the PVDF major loop simulated using these parameters is compared with the experimental major loop in Fig. 4.[11,18] We see that the parameters are chosen such that all the experimental loops lie inside the simulated loop because we assume that minor loops are all within the interior of the major loop.[1]
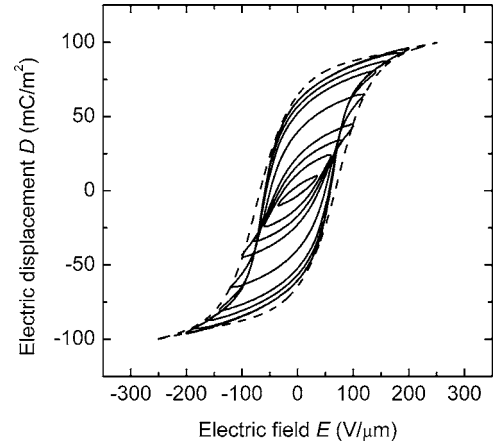

FIG. 4. D-E loop of a uniaxially drawn PVDF at 20 °C. The simulation result (dashed lines) based on the superposition Preisach model is compared with the experimental results in Ref. 11 (solid lines).

Figure 5(a) shows the simulated permittivity following the methodology in Sec. III A 1. Also included is the experimental permittivity.[11] We see that almost all features of the experimental curve can be reproduced.

In Fig. 5(b), we show an "alternative" calculation. An electric field $E = E_0 \cos(2\pi ft)$ is applied to the copolymer sample with frequency $f=0.8$ Hz and magnitude $E_0 = 200$ V μm^{-1}. The simulated dielectric constant is obtained by using an alternative definition of permittivity (i.e., the derivative of D with respect to the electric field E, commonly adopted by many authors). It is seen that this simulated curve cannot reproduce the experimental magnitudes. We can conclude that the experimental permittivity is not equal to the widely accepted "theoretical permittivity."
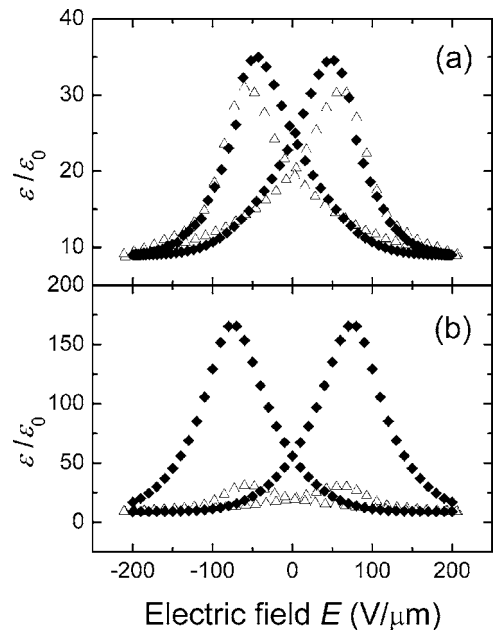

FIG. 5. The simulated electric-field dependence of permittivity of PVDF (diamond symbols) is compared with the experimental data in Ref. 11 (triangular symbols). (a) Results calculated by using the measuring method in Sec. III A. (b) Results calculated based on the definition of permittivity $\varepsilon \equiv dD/dE$.
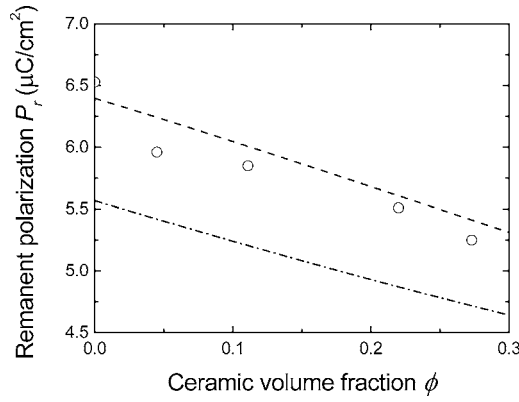
FIG. 6. The remanent polarization P_r of the TGS / P(VDF-TrFE) composite with different values of the volume fraction ϕ of TGS. The simulation results based on the present model (dashed lines) and the Miller model (dashed-dotted lines) are compared with the experimental results in Ref. 12 (open symbols).

B. Prediction of remanent polarization in TGS/P(VDF-TrFE) 0-3 composite

In this section, our model and the Miller model are separately applied to simulate the P-E responses in the constituent material within TGS/P(VDF-TrFE) 0-3 composites subjected to poling by a full cycle of an ac field.[12] The simulated remanent polarization values with different TGS content are compared with the experimental results. In this work, we only focus on composites with low TGS content.

We consider a composite comprising a dilute dispersion of spherical particles of permittivity ε_i and polarization P_i in a matrix of permittivity ε_m and polarization P_m. The local electric fields E_i and E_m acting on the inclusion and matrix phases may be written as (see Appendix B)

$$E_i = \frac{3\varepsilon_m E + (1-\phi)(P_m - P_i)}{\phi\, 3\varepsilon_m + (1-\phi)(\varepsilon_i + 2\varepsilon_m)}, \quad (17)$$

and

$$E_m = \frac{E - \phi\, E_i}{1 - \phi}, \quad (18)$$

given the external electric field E, which, for the present purpose, is a sinusoidal field. In Eq. (17), ϕ is the volume fraction of the inclusion phase. A hysteresis model should be adopted for the P-E relations of the constituent phases. Then the electric displacement of the composite can be calculated from
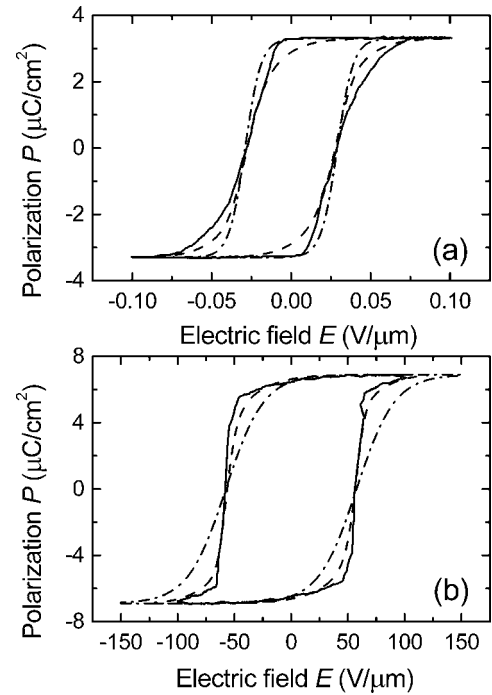

FIG. 7. P-E loop of (a) TGS and (b) P(VDF-TrFE) at room temperature. The simulation results based on the present model (dashed lines) and the Miller model (dashed-dotted lines) are compared with the experimental results in Ref. 12 (solid lines).

$$D = \phi D_i + (1 - \phi)D_m, \quad (19)$$

where $D_i = \varepsilon_i E_i + P_i$ and $D_m = \varepsilon_m E_m + P_m$.

Since our superposition Preisach model can provide an analytic form for arbitrary P_i-E_i and P_m-E_m relations [see Eqs. (4)–(9)], the local electric fields E_i and E_m can be solved by using Eqs. (17) and (18). However, the Miller model is a differential hysteresis model,[1] thus a system of differential equations must be tackled for the simulation of polarization under an applied field history.

In Ref. 12, the 0-3 composites of TGS/[P(VDF-TrFE) in the composition 70/30 mol %] with small volume fractions of TGS are "polarized" by applying a few cycles of a 100 V μm^{-1} sinusoidal field of 10 Hz at room temperature. The remanent polarization P_r of the 0-3 composites obtained from the measured hysteresis loop is shown in Fig. 6. It shows that the remanent polarization P_r decreases with volume fraction ϕ.

The dielectric and ferroelectric properties as well as the Preisach parameters (k_i and ν_i) adopted in this simulation for

TABLE II. The dielectric and ferroelectric properties as well as the Preisach parameters k_i and ν_i of the TGS and P(VDF-TrFE) used in Figs. 6–8.

	ε_r	P_s (μC cm^{-2})	P_r (μC cm^{-2})	E_c (V μm^{-1})	k_1	ν_1 (V μm^{-1})	k_2	ν_2 (V μm^{-1})	k_3	ν_3 (V μm^{-1})
TGS	31.15[a]	3.33[b]	3.28[b]	0.029[b]	0.55	0.013	0.45	0.037	⋯	⋯
P(VDF-TrFE)	12.45[c]	6.9[b]	6.5[b]	57.6[b]	0.65	10	0.2	40	0.15	50

[a]The dielectric constant of TGS powder is calculated from the modified Bruggeman formula, (Ref. 19) $1 - 1/\varepsilon_r = (\varepsilon_a - 1)/(2\varepsilon_r + \varepsilon_a) + (\varepsilon_b - 1)/(2\varepsilon_r + \varepsilon_b) + (\varepsilon_c - 1)/(2\varepsilon_r + \varepsilon_c)$, with $\varepsilon_a = 12.8$ (see Ref. 20), $\varepsilon_b = 130$ (see Ref. 21), and $\varepsilon_c = 11.3$ (see Ref. 20).
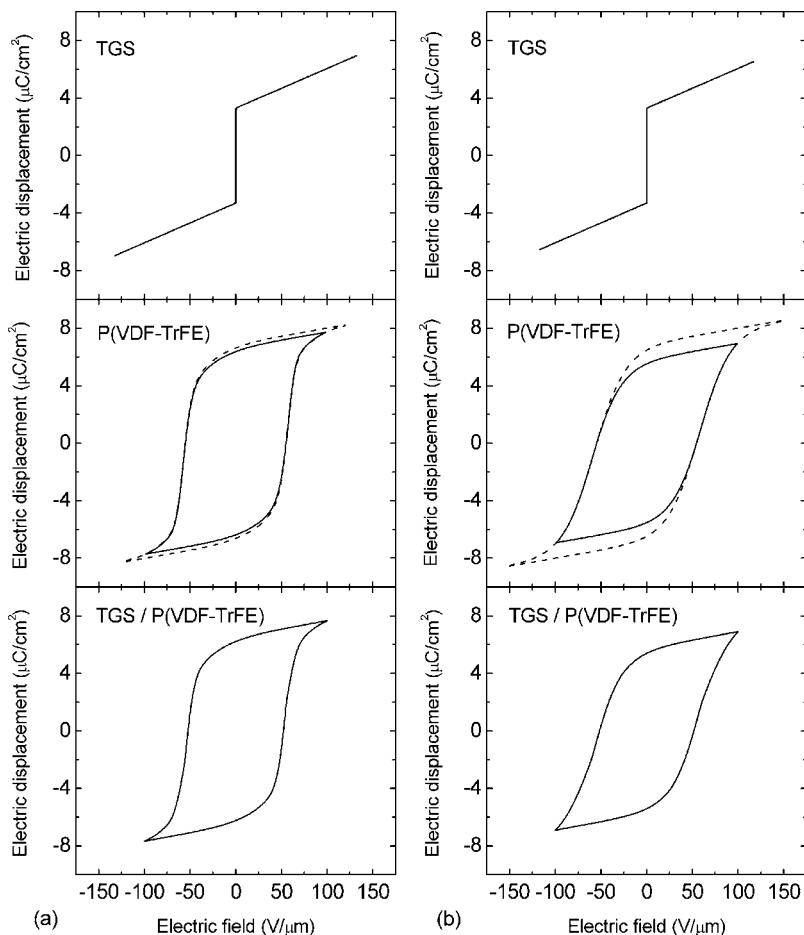[b]Reference 12.
[c]Reference 18.

FIG. 8. The solid lines denote the simulated *D-E* history in the constituent material and TGS/P(VDF-TrFE) composite during poling of the composite. The dotted lines denote the simulated major loops, respectively, of the constituent material. (a) The present model and (b) the Miller model.

TGS and P(VDF-TrFE) are given in Table II. Using both our model and the Miller model, the simulated *D-E* major loops of TGS and P(VDF-TrFE) are calculated and Fig. 7 shows their comparison with the experimental data. It shows that our model results give a better fit with the shape of the experimental loops than the Miller model does. The P_r values obtained from the simulated loops of TGS/P(VDF-TrFE) composites are compared with the experimental results in Fig. 6.[12] Our model predictions agree better with the experimental results.

In the following, we choose the case of $\phi = 0.05$ as an example to demonstrate the relative merits of our model. The *D-E* behavior calculated for each constituent material in the ac poling is shown in Fig. 8. In both models, the TGS can be fully polarized under the adopted poling field. For P(VDF-TrFE), the local field E_m in our model is sufficiently large for a complete polarization, but in the Miller model E_m is not sufficient and only a minor loop is traced during the process [see Fig. 8(b)]. According to the experiment, a fully polarized matrix phase can be obtained when $E_m \geq 100$ V/μm [see Fig. 7(b)]. Since E_m goes up to roughly ± 100 V/μm in both models [see Fig. 8(b)], the calculated remanent polarization P_{rm} of the matrix should be very close to 6.5 μC/cm^2 (see Table II). This can be reproduced by our model. However, the prediction given by the Miller model is only 5.5 μC/cm^2, which is significantly lesser than the "true value." This is due to the fact that the major loop described by the Miller model is difficult to fit well with the experi-

mental loop of the copolymer, and large discrepancy between their shapes is noted [see Fig. 7(b)]. According to the calculation with the Miller model, an electric field of $E_m \approx 150$ V/μm is required to get $P_{rm} \approx 6.5$ μC/cm^2. As a result, for all volume fractions under investigation, the remanent polarization values after the poling obtained by the Miller model are significantly lower than the experimental results (see Fig. 6). This shows that an accurate description of the shape of the major loop is important in the studies of polarization.

IV. DISCUSSION

Recall that minor loops in the Miller model are calculated by scaling the major loop.[1] Although the structure of the Miller model is simple, the simulated minor loops show strong unstable phenomena,[2] probably due to an insufficient consideration of history-dependent effects. To show this shortcoming, we consider a polarizing process for a ferroelectric polymer shown in Fig. 9(a). The parameters of the Miller model, including the coercive field, remanent polarization, and spontaneous polarization, are chosen as shown in Table III. We first assume that the material is subjected to an initial field of -300 V μm^{-1}, and its initial polarization is negatively saturated. Then, a cyclic field with small magnitude, shown in Fig. 9(a), is applied to the material and the calculated *P-E* curve is shown in Fig. 9(b). It is obvious that the *P-E* curve cannot form a closed hysteresis loop and
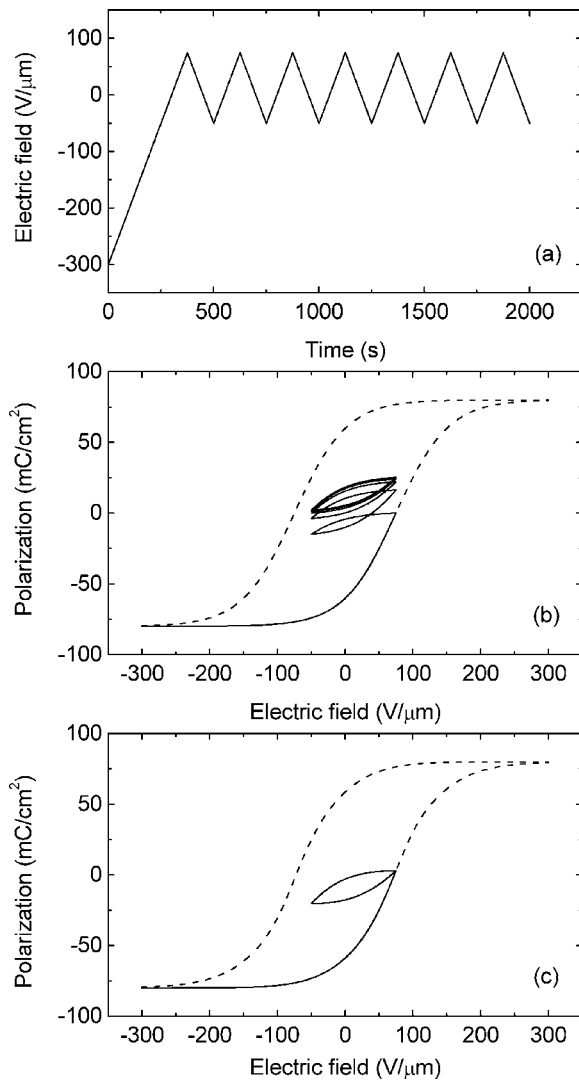
FIG. 9. (a) A field history is applied to a ferroelectric polymer in a poling process. Simulated hysteresis loops using (b) the Miller model, and (c) the present model. The solid and dashed lines denote the P-E history during the poling process and the major loop of the polymer, respectively.

different hysteresis loop shapes even though they have the same values of E_c, P_r, and P_s. Our superposition Preisach model can provide a greater freedom to describe the hysteresis loop of ferroelectrics (Sec. II B). This is important when applying the hysteresis model to other studies such as that demonstrated in Sec. III B, which shows the shape of the major hysteresis loop significantly affecting the prediction of effective polarization in composites.

V. CONCLUSIONS

In conclusion, the use of the Preisach function in the form of Eq. (3) together with the superposition method introduced in Sec. II B allows us to obtain explicit expressions for arbitrary polarization reversal curves, the virgin curve, and major loop of ferroelectrics. Using this technique, it is convenient to simulate the experimental ascending and descending polarization profiles of the major loop of a ferroelectric. The simulated polarization curve under arbitrary field history can also be expressed in analytical formulas. This model also retains the characteristic properties of the Preisach model, e.g., deletion property, congruency property, and stable hysteresis loops (Sec. IV).

The model is useful for the investigation of the electric field dependence of the dielectric permittivity and the remanent polarization of 0-3 composites. For the case of dielectric permittivity, we find that the dielectric permittivity obtained experimentally cannot be simply taken as dD/dE on the major hysteresis loop. In other words, consideration of the unsaturated loops is essential to model the measured permittivity. For the case of 0-3 composites, our simulation gives more realistic P_r values. We find that an accurate expression for the shape of the major loop of constituent materials in a composite is quite important. It seems that our model shows some advantages in studies involving ferroelectric hysteresis over the Miller model.

"moves" upward. This instability property has yet to find experimental support and is likely unrealistic. In Fig. 9(c), the Preisach parameters (see Table III) are chosen such that the major loop of our model can fit well with the shape of the corresponding Miller loop. Our calculated P-E curve under the same schedule of applied field [Fig. 9(a)] is shown in Fig. 9(c). It is seen that this P-E curve does not "drift" and forms a closed minor loop. Actually, the formation of closed P-E loops is commonly observed.[2,15–17]

The Miller model only has three parameters: coercive field E_c, remanent polarization P_r, and spontaneous polarization P_s. However, different kinds of ferroelectrics may have

TABLE III. The ferroelectric properties as well as the Preisach parameters k_i and ν_i of a polymer used in Fig. 9.

P_s (mC cm^{-2})	P_r (mC cm^{-2})	E_c (V μm^{-1})	k_1	ν_1 (V μm^{-1})	k_2	ν_2 (V μm^{-1})	k_3	ν_3 (V μm^{-1})	k_4	ν_4 (V μm^{-1})
80	60	75	0.2	40	0.1	80	0.5	120	0.2	170

APPENDIX A

The polarization of the ascending major curve is

$$P_{\text{sat}}^+(E;h,\nu) = -P_s + 2P_s \int_{-\infty}^{E} \int_{-\infty}^{U} \wp(U,V;h,\nu)dVdU$$

$$= \frac{P_s f}{8} \left\{ 2 \coth\left(\frac{2h}{\nu}\right) \left[4 \operatorname{csch}^2\left(\frac{2h}{\nu}\right) \ln\left(\frac{\cosh[(E-h)/\nu]}{\cosh[(E+h)/\nu]}\right) + \operatorname{sech}^2\left(\frac{E-h}{\nu}\right) \right] + 4 \coth^3\left(\frac{2h}{\nu}\right)\tanh\left(\frac{E-h}{\nu}\right) \right.$$

$$+ \operatorname{csch}^2\left(\frac{2h}{\nu}\right)\left[\left(2 + 4\cosh\left(\frac{4h}{\nu}\right)\right)\operatorname{csch}^2\left(\frac{2h}{\nu}\right)\ln\left(\frac{\cosh[(E-h)/\nu]}{\cosh[(E+h)/\nu]}\right) + \cosh\left(\frac{4h}{\nu}\right)\operatorname{sech}^2\left(\frac{E-h}{\nu}\right) + 2\left(\operatorname{sech}\left(\frac{2h}{\nu}\right)\right.\right.$$

$$\left.\left.\left. + \operatorname{csch}\left(\frac{2h}{\nu}\right)\right)\operatorname{sech}\left(\frac{E+h}{\nu}\right)\sinh\left(\frac{E-h}{\nu}\right) + 2\left(2 + \cosh\left(\frac{4h}{\nu}\right)\right)\tanh\left(\frac{E-h}{\nu}\right)\right]\right\}, \tag{A1}$$

where

$$f = \frac{-8\exp(-4h/\nu)\,\nu\,\sinh^4(2h/\nu)}{8h - 2\nu + 2(2h+\nu)\cosh(4h/\nu) - (4h+3\nu)\sinh(4h/\nu)} \tag{A2}$$

denote the normalized factor. The polarization of the virgin curve is

$$P_0^+(E;h,\nu) = 2P_s \int_0^E \int_{-U}^{U} \wp(U,V;h,\nu)dVdU$$

$$= \frac{P_s f}{16} \left\{ 64 e^{(8h)/\nu}\left(1 + 2e^{(4h)/\nu}\right)\left(1 - e^{(4h)/\nu}\right)^{-4}\ln\left\{\frac{\cosh[(E-h)/\nu]}{\cosh[(E+h)/\nu]}\right\} + \operatorname{sech}^2\left(\frac{E-h}{\nu}\right)\left[2\coth\left(\frac{2h}{\nu}\right)\left(2 + \coth\left(\frac{2h}{\nu}\right)\right)\right.\right.$$

$$\left. - 6 + \operatorname{sech}^2\left(\frac{E-h}{\nu}\right) + 4\tanh\left(\frac{E-h}{\nu}\right)\right] + \operatorname{csch}^3\left(\frac{2h}{\nu}\right)\left[2\left(3\cosh\left(\frac{2h}{\nu}\right) + \cosh\left(\frac{6h}{\nu}\right) + 6\sinh\left(\frac{2h}{\nu}\right)\right)\tanh\left(\frac{E-h}{\nu}\right)\right.$$

$$\left.\left. + 4\operatorname{sech}\left(\frac{E+h}{\nu}\right)\sinh\left(\frac{E-h}{\nu}\right)\left(1 + \tanh\left(\frac{2h}{\nu}\right)\right)\right]\right\}. \tag{A3}$$

If the applied field E increases from E_0 to $E_0 \leq E < E_1$, then the change in the polarization is

$$\Delta P^+(E,E_0;h,\nu) = 2P_s \int_{E_0}^{E} \int_{E_0}^{U} \wp(U,V;h,\nu)dVdU = \frac{P_s f}{32}\operatorname{csch}^2\left(\frac{2h}{\nu}\right)\left\{8\left(1 + 4\coth\left(\frac{2h}{\nu}\right)\right.\right.$$

$$\left. + 3\coth^2\left(\frac{2h}{\nu}\right)\right)\ln\left(\frac{\cosh[(E-h)/\nu]\cosh[(E_0-h)/\nu]}{\cosh[(E+h)/\nu]\cosh[(E_0+h)/\nu]}\right) + 16e^{(2h)/\nu}\operatorname{csch}\left(\frac{4h}{\nu}\right)\left[\operatorname{sech}\left(\frac{E+h}{\nu}\right)\sinh\left(\frac{E-h}{\nu}\right)\right.$$

$$\left. + \operatorname{sech}\left(\frac{E_0+h}{\nu}\right)\sinh\left(\frac{E_0-h}{\nu}\right)\right] - 4\cosh\left(\frac{-E_0+h}{\nu}\right)\left[\operatorname{sech}\left(\frac{E-h}{\nu}\right)\operatorname{sech}^2\left(\frac{E_0+h}{\nu}\right)\right.$$

$$\left. + \frac{4}{(\cosh[(2E_0)/\nu] + \cosh[(2h)/\nu])^2}\right] \times \left[\cosh\left(\frac{E_0+3h}{\nu}\right) + 2\cosh\left(\frac{E_0+h}{\nu}\right)\sinh\left(\frac{2h}{\nu}\right)\right]$$

$$+ \operatorname{csch}\left(\frac{2h}{\nu}\right)\operatorname{sech}^2\left(\frac{E_0+h}{\nu}\right)\left(\tanh\left(\frac{E-h}{\nu}\right) - \tanh\left(\frac{E_0-h}{\nu}\right)\right)\left[e^{(2E_0-4h)/\nu} + e^{-(2E_0-2h)/\nu} - 3e^{(2E_0)/\nu} + 6e^{(2h)/\nu}\right.$$

$$\left.\left. + 2e^{(6h)/\nu} + 3e^{-(2E_0)/\nu} + 6e^{(2E_0+4h)/\nu}\right]\right\}. \tag{A4}$$

APPENDIX B

We first write the electric displacement D for the ferroelectric constituent materials in the composite as

$$D_i = \varepsilon_i E_i + P_i,$$

$$D_m = \varepsilon_m E_m + P_m,$$

(B1)

where P is the polarization, ε denotes the permittivity, and E is the electric field. Subscripts i and m denote "inclusion" and "matrix," respectively.

Consider the single inclusion problem of a ferroelectric sphere surrounded by a ferroelectric matrix medium with a uniform electric field applied along the z direction far away from the inclusion. The boundary value problem gives the following equations:[22]

$$D_i + 2\varepsilon_m(E_i - E_m) = D_m.$$

(B2)

In Eq. (B2), we have assumed both constituent materials are uniformly polarized.

For a composite comprising a dilute suspension of spherical particles uniformly distributed in the matrix material, the electric fields satisfy

$$E = \phi E_i + (1 - \phi)E_m,$$

(B3)

where ϕ is the volume fraction of the inclusion phase. We obtain from Eqs. (B1)–(B3),

$$E_i = \frac{3\varepsilon_m E + (1 - \phi)(P_m - P_i)}{\phi 3\varepsilon_m + (1 - \phi)(\varepsilon_i + 2\varepsilon_m)}.$$

(B4)

[1] S. L. Miller, J. R. Schwank, R. D. Nasby, and M. S. Rodgers, J. Appl. Phys. **70**, 2849 (1991).
[2] B. Jiang, J. C. Lee, P. Zurcher, and R. E. Jones, Jr., Integr. Ferroelectr. **16**, 805 (1997).
[3] F. Preisach, Z. Phys. **94**, 277 (1935).
[4] A. V. Turik, Sov. Phys. Solid State **5**, 885 (1963).
[5] G. Robert, D. Damjanovic, and N. Setter, Appl. Phys. Lett. **77**, 4413 (2000).
[6] A. T. Bartic, D. J. Wouters, H. E. Maes, J. T. Rickes, and R. M. Waser, J. Appl. Phys. **89**, 3420 (2001).
[7] C. H. Tsang, B. Ploss, B. Ploss, and F. G. Shin, Ferroelectrics **259**, 139 (2001).
[8] R. G. Mendes, I. A. Santos, E. B. Araújo, and J. A. Eiras, Ferroelectrics **271**, 1837 (2002).
[9] M. Maleto, E. Pevtsov, A. Sigov, and A. Svotina, Ferroelectrics **286**, 1023 (2003).
[10] H. Maiwa and N. Ichinose, Jpn. J. Appl. Phys., Part 1 **42**, 4392 (2003).
[11] T. Furukawa, K. Nakajima, T. Koizumi, and M. Date, Jpn. J. Appl. Phys., Part 1 **26**, 1039 (1987).
[12] Y. Yang, M. Phil. thesis, The Hong Kong Polytechnic University, 2005.
[13] V. Meyer, J.-M. Sallese, P. Fazan, D. Bard, and F. Pecheux, Solid-State Electron. **47**, 1479 (2003).
[14] I. D. Mayergoyz, *Mathematical Models of Hysteresis* (Springer-Verlag, New York, 1991).
[15] P. Ge and M. Jouaneh, Precis. Eng. **17**, 211 (1995).
[16] P. Ge and M. Jouaneh, Precis. Eng. **20**, 99 (1997).
[17] D. Hughes and J. T. Wen, Smart Mater. Struct. **6**, 287 (1997).
[18] T. Furukawa, Phase Transitions **18**, 143 (1989).
[19] A. Mansingh and S. S. Bawa, J. Phys. Soc. Jpn. **35**, 1136 (1973).
[20] Yu. M. Poplavko, L. P. Pereverzeva, P. I. Yashchishin, V. V. Meriakri, E. F. Ushatkin, and S. V. Ogurtsov, Ukr. Fiz. Zh. (Russ. Ed.) **19**, 1688 (1974).
[21] Yu. M. Poplavko, L. P. Pereverzeva, V. V. Meriakri, E. F. Ushatkin, S. V. Ogurtsov, and P. I. Yashchishin, Sov. Phys. Solid State **15**, 842 (1973).
[22] C. K. Wong, Y. M. Poon, and F. G. Shin, J. Appl. Phys. **90**, 4690 (2001).